

## LOW RATES OF FATIGUE CRACK GROWTH IN BETA HEAT TREATED TITANIUM ALLOY

M.D. Halliday

Department of Physical Metallurgy and Science of Materials,  
University of Birmingham, P.O. Box 363, Birmingham B15 2TT, U.K.

### ABSTRACT

Crack closure was found to be present during fatigue crack growth in the titanium alloys IMI 318 and IMI 685 after  $\beta$  heat treatment. Internal stresses induced by heat treatment and tests at different R ratios produced, in the presence of crack closure, considerable scatter in the crack growth data for IMI 685. Crack closure was related to mismatch across the fracture faces due to the highly irregular crack path. Both the range of growth rates found in the IMI 685 and differences in growth rate between the two alloys were rationalized by an effective  $\Delta K$  parameter. A comparison of the growth rates in IMI 318 in the mill annealed and  $\beta$  heat treated conditions showed that the relatively low growth rates after  $\beta$  heat treatment could only be partly explained by crack closure.

### KEYWORDS

Fatigue crack growth; titanium alloy; beta heat treatment; crack closure; internal stress.

### INTRODUCTION

Several recent papers have compared the fatigue crack growth resistance of titanium alloys for heat treatments above and below the  $\beta$  transus. They provide substantial evidence that microstructures produced by  $\beta$  heat treatment are associated with relatively low crack growth rates (Chesnutt, Rhodes and Williams, 1976; Evans, 1973; Evans and Beale, 1978; Eylon and co-workers, 1976; Halliday and Beevers, 1979; Harrigan and co-workers, 1974; Neal, 1978; Paton and co-workers, 1975; Yoder and co-workers, 1977a, 1977b, 1979a). The growth rates for the same alloy can show a large scatter however, (Eylon and co-workers, 1976) and for different alloys can cover a wide range (Yoder, Cooley and Crooker, 1979a).  $\beta$  heat treated material is usually characterized by a microstructure with an acicular  $\alpha$  phase morphology and by a remarkably irregular fatigue fracture path. Explanations for the low growth rates have included crack diversion at the  $\alpha$  plates (Evans, 1973), secondary cracking at  $\alpha$ - $\beta$  interfaces (Chesnutt and co-workers, 1976), microstructure controlled crack growth when the reverse plastic zone size is less than the  $\alpha$  colony size (Yoder, Cooley and Crooker, 1977a, 1979a, 1979b) and crack branching (Eylon and Bania, 1978; Eylon and co-workers, 1976; Postans and Jeal, 1978). In

addition, it was suggested in a recent note that contact stresses across the irregular fracture faces could produce reduced crack growth rates (Halliday and Beevers, 1979). Further work has now been performed to examine this mechanism and is reported here.

EXPERIMENTAL

Fatigue crack growth tests were performed on the titanium alloys Ti-6Al-4V (IMI 318) and Ti-6Al-5Zr-0.5Mo-0.25Si (IMI 685). Compact tension specimens, CTS, were used of thickness 20mm and width 40mm. Manufacturer's chemical analyses of the alloys are given in Table 1.

TABLE 1 Chemical Analyses of the Alloys (wt %)

	Al	V	Zr	Mo	Si	Fe	O <sub>2</sub>	N <sub>2</sub>	H <sub>2</sub>	Ti
IMI 318	6.50	4.30				0.05	0.16	<0.02	0.002	Bal.
IMI 685	6.20		5.22	0.51	0.24	0.02	0.13	<0.01	0.007	Bal.

IMI 685 is a mainly  $\alpha$  phase alloy which is  $\beta$  heat treated and has useful creep properties at service temperatures up to about 550°C. In the as-received condition the final heat treatment was at 1050°C followed by oil quench, 24hr at 550°C and air cool. Ageing temperature is usually in the range 550°C to 580°C to achieve an optimum combination of tensile and creep properties. The microstructure of the IMI 685 depends upon cooling rate after solution treatment and in large sections a range of structures can be expected. Slow cooling rates produce large colonies of coarse, aligned Widmanstätten laths and with rapid quenching the  $\alpha$  forms by a martensitic transformation. After intermediate cooling rates, basketweave  $\alpha$  of varying degrees of coarseness is produced by Widmanstätten nucleation and growth. To examine the fatigue crack growth properties of a range of structures which could be produced within a component by a nominal oil quench, some blanks for test specimens were re-heat treated. The blanks were heated in air but were oversize so that 2.5mm was removed from the surfaces in the final machining. They were given a common solution treatment of 1/2 hr at 1050°C followed by furnace cooling, oil quenching or water quenching. Two alternative ageing treatments of 24hr at 550°C and 24hr at 580°C were also used and in addition one oil quenched blank was annealed for 24 hr at 700°C.

IMI 318 is an  $\alpha+\beta$  alloy and was supplied mill annealed (final working high in  $\alpha+\beta$  phase field, 2hr at 700°C, air cool). Some of the alloy was given a treatment of 1/2 hr at 1050°C, oil quench, 2 hr at 700°C, air cool to examine the influence of  $\beta$  heat treatment on fatigue crack growth resistance compared with mill anneal. Crack growth was monitored in the mill annealed IMI 318 using a d.c. potential drop method and in the other specimens from change in compliance as measured by a crack mouth displacement gauge. Contact across the crack faces during the fatigue cycle was examined from both the p.d. and displacement gauge output. Fatigue testing was performed in load control on a servo-hydraulic Instron Dynamic Testing Instrument at R ratios of 0.1 and 0.7.

RESULTS AND DISCUSSION

The fatigue crack growth results for the tests on IMI 685 at R 0.1 are shown in Fig. 1 in terms of growth rate as a function of  $\Delta K$  determined from the applied load

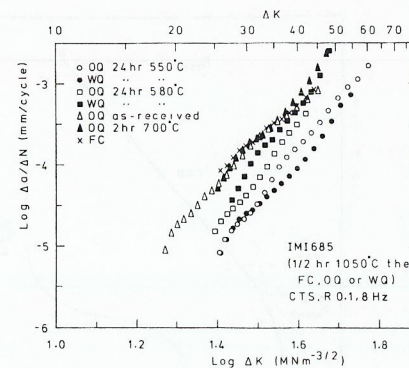


Fig. 1. Range of fatigue crack growth rates at R 0.1 in IMI 685 as a function of  $\Delta K$ .

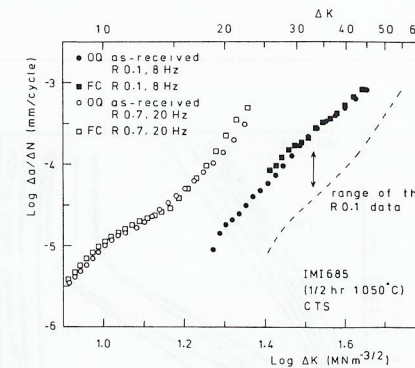


Fig. 2. Dependence of fatigue crack growth rate on R ratio in IMI 685.

range. It is seen that the spread in growth rates for the different heat treatments covered a range of about  $\times 10$ . The Fig. also shows that the highest growth rates were in the furnace cooled material and that water quenching and ageing at 550°C gave the lowest growth rate. The growth rate after water quenching was increased by ageing at 580°C and the oil quenched specimens also showed a similar effect of ageing temperature. Crack growth rates in the as-received oil quenched material were similar to those in the furnace cooled specimen as were those after oil quenching and annealing at 700°C. The slopes of the curves gave an m value of about 5.2 in the well known Paris-Erdogan (1963) relationship

$$\Delta a/\Delta N = A \Delta K^m \tag{1}$$

High values of m for crack growth at intermediate rates in  $\beta$  heat treated titanium alloys have been considered to arise due to static fracture processes (Evans and Beale, 1978) and due to microstructure sensitive fatigue crack growth (Yoder and co-workers, 1977).

The scatter in the growth rates was not only a function of heat treatment however, but was also dependent upon the mean load in the fatigue cycle. This is shown in Fig. 2 where tests on furnace cooled and as-received material are compared for R ratios of 0.1 and 0.7. The similarity in growth rates between the two material conditions at R 0.1 was again evident at R 0.7. It is appreciated that as  $\Delta K$  is increased the growth data for R 0.7 will diverge from that at R 0.1 because of the approach of fast fracture. The results in Fig. 2 show however, that even at  $\Delta K$  values below where this is expected to be important, the growth rate at R 0.7 was significantly higher than that at R 0.1. Most fatigue crack growth work on  $\beta$  heat treated titanium alloy has been carried out at one R ratio, usually 0.1, but where different R ratios were used it was found that growth rate was greater at the higher R ratio (Evans and Beale, 1978). The lowest growth rates from Fig. 1 are reproduced in Fig. 2 by the dotted line so that the full range of the growth rates due to heat treatment and R ratio may be seen in the one Fig.

Crack mouth opening/load and p.d./load curves recorded at intervals during the above fatigue tests showed that load transfer occurred across the crack faces during fatigue at R 0.1 but not at R 0.7. An example of the recordings is shown in Fig. 3; the p.d. output is from the full load cycle but the COD output only

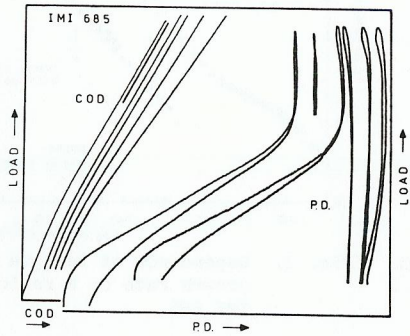


Fig. 3. Experimental load/COD and load/p.d. traces obtained during fatigue crack growth in  $\beta$  heat treated IMI 685.

shows the loading part of the cycle. The potential drop method was found to give inconsistent and generally higher values of crack opening load and this was considered to occur because the electrical resistance method is sensitive to rubbing contact whilst the COD method only responds to load bearing contact. Values of crack opening load were therefore obtained only from the COD results. Load transfer across the crack was shown not to be a surface effect by introducing

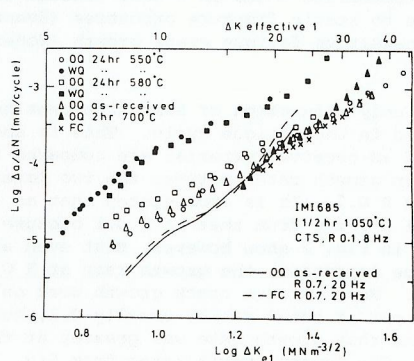


Fig. 5. Fatigue crack growth rates in IMI 685 as a function of an effective  $\Delta K$  parameter obtained from the crack opening load,  $P_{open 1}^{COD}$ .

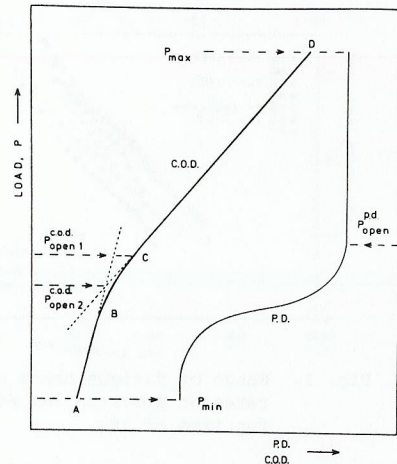


Fig. 4. Schematic showing the derivation of crack closure loads from COD and p.d. traces.

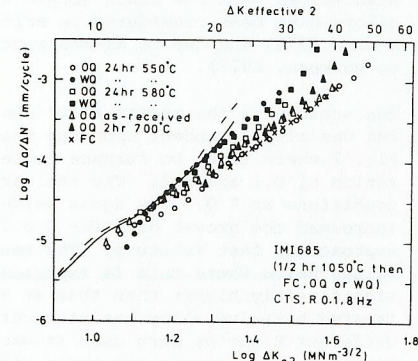


Fig. 6. Fatigue crack growth rates in IMI 685 as a function of an effective  $\Delta K$  parameter derived from the load at the intersection of tangents to the load/COD curve,  $P_{open 2}^{COD}$ .

grooves to a depth of 12% of the thickness along the intersection of the crack plane with the side faces part way through a test on as-received material. The decrease in crack opening load produced by the side grooves was only of the size expected from the decrease in specimen thickness. The levels of crack closure in the test at R 0.1 showed a trend which was consistent with the crack growth results and was lowest in the high crack growth rate specimens and highest in the low rate ones.

The results at R 0.7 in Fig. 2 show that the furnace cooled and oil quenched microstructures have similar resistance to fatigue crack growth over the intermediate growth rate range in the absence of crack closure. It was also shown in Fig. 1 that furnace cooled, as-received oil quenched and oil quenched and annealed at 700°C material had the same growth rate at R 0.1. This suggests that the range of growth rates at R 0.1 was largely due to internal stresses which were left in the laboratory quenched material after ageing at 550°C or 580°C. The as-received oil quenched IMI 685 was aged at 550°C but the industrial quench would have been less severe than the nominally similar laboratory quench due to section size and transfer time and also an unknown but probably relatively large amount of surface material was removed. For the above reasons it is not surprising that the as-received material was comparatively free from thermal stresses and gave a similar crack growth response to the furnace cooled specimen. The results clearly indicate however, a source of variability in crack growth rates which can occur in these alloys.

The difference in growth rates for the material at R 0.7 and R 0.1 shown in Fig. 2 is considered to arise from closure effects uncomplicated by thermal stresses. Elber (1970), first demonstrated the presence of crack closure during work on an aluminium alloy. He suggested that the effective load range during fatigue when closure occurred was the load range for which the crack was fully open. This is shown as region CD of the COD curve in Fig. 4 which gives schematic responses of the COD and p.d. to crack closure. The crack is fully closed over region AB of the curve. Elber's suggestion therefore defines an effective  $\Delta K$  which by reference to Fig. 4 becomes

$$\Delta K \text{ effective } 1 = \Delta K \frac{(P_{max}^{COD} - P_{open 1}^{COD})}{(P_{max} - P_{min})} \quad (2)$$

The fatigue crack growth data shown in Figs. 1 and 2 was re-interpreted in terms of an effective  $\Delta K$  defined by equation (2) and is presented in Fig. 5. It is clear that the  $\Delta K$  effective given by equation (2) does not lead to a satisfactory description of the results. The scatter was not reduced and crack growth at R 0.7 was presented as being more difficult than at R 0.1 for the same heat treatment, which is very unlikely. Closure in the Elber model arises from the wedging action of the plastically deformed layer left in the wake of the crack and occurs from the crack tip backwards at the load equivalent to  $P_{open 1}^{COD}$  on the unloading part of the cycle. It is suggested however, that load transfer across the crack in the present materials arises from the irregular nature of the fracture path as exemplified in Fig. 6. In this model the tortuosity and branching of the crack which is commonly found in  $\beta$  heat treated titanium alloys produces mismatch of the fracture faces across the plane of the crack and contact on unloading occurs behind the crack tip as shown for example in Fig. 7. (Halliday and Beevers, 1979). The crack tip therefore remains open and some of the load range below that at which contact across the crack faces first occurs,  $P_{open 1}^{COD}$  is expected to contribute to crack growth. Walker and Beevers (1979), found a similar mechanism for closure also satisfied their observations of fatigue cracking in commercially pure titanium.

A second crack opening load,  $P_{open 2}^{COD}$ , may be defined as shown in Fig. 4 and may be

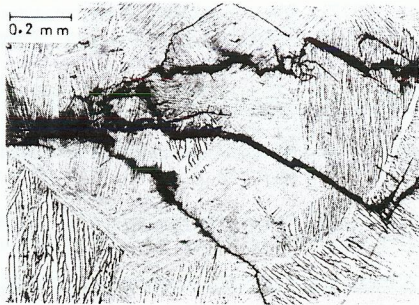


Fig. 7. Example micrograph of the branched and tortuous crack path in IMI 685. Furnace cooled after  $\beta$  heat treatment, nominal crack plane horizontal.

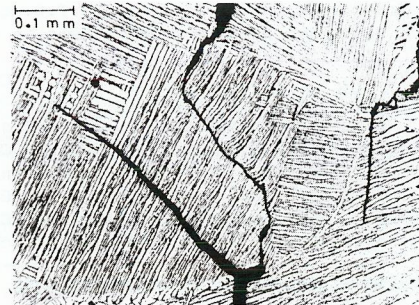


Fig. 8. Micrograph of load bearing contact across the crack faces at a point behind the crack tip in furnace cooled IMI 685. Note the distortion of the  $\alpha$  platelets. Nominal crack plane vertical.

chosen empirically as the lower effective load in the fatigue cycle so that

$$\Delta K \text{ effective } 2 = \Delta K (P_{\max} - P_{\text{open } 2}^{\text{COD}}) / (P_{\max} - P_{\min}) \quad (3)$$

The fatigue crack growth rates from Figs. 1 and 2 are described in terms of  $\Delta K$  effective 2 in Fig. 8. It is seen that the results now fall in a relatively narrow scatter band with slope  $m$  in equation (1), if  $\Delta K$  is replaced by  $\Delta K$  effective 2, of  $\sim 3.8$  which is more typical of the values found for intermediate fatigue crack growth rates.

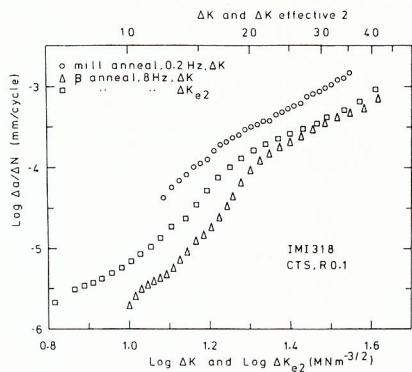


Fig. 9. Comparison of fatigue crack growth rates at R O.1 in mill annealed and  $\beta$  annealed IMI 318 as a function of  $\Delta K$ . The  $\beta$  annealed crack growth data are also presented in terms of an effective  $\Delta K$  parameter obtained from  $P_{\text{open } 2}^{\text{COD}}$ .

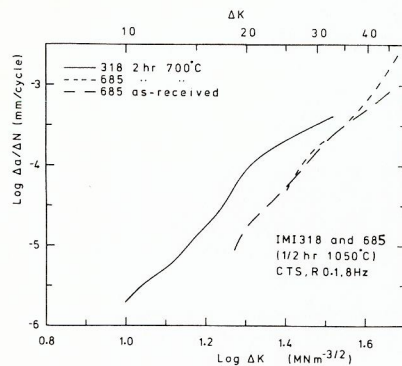


Fig. 10. Comparison of fatigue crack growth rates at R O.1 in oil quenched IMI 318 and IMI 685 as a function of  $\Delta K$ .

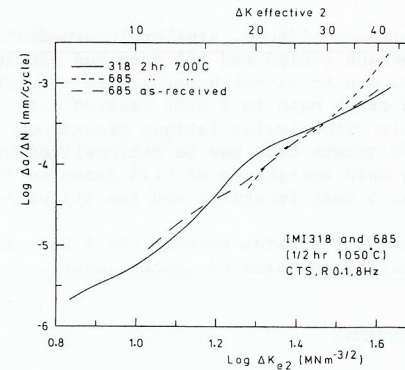


Fig. 11. Comparison of fatigue crack growth rates at R O.1 in oil quenched IMI 318 and IMI 685 as a function of an effective  $\Delta K$  parameter obtained from  $P_{\text{open } 2}^{\text{COD}}$ .

Equation (3) was also fitted to the crack growth data obtained from the tests on IMI 318. Figure 9 shows the crack growth rates for mill annealed material and  $\beta$  heat treated material at R O.1 as a function of  $\Delta K$ . The crack growth results for the  $\beta$  heat treated test are also given in terms of  $\Delta K$  effective 2. The improvement in crack growth resistance due to  $\beta$  heat treatment compared with mill anneal is demonstrated in Fig. 9 which also shows that the improvement cannot be attributed entirely to crack closure through equation (3). Crack closure was not found in mill annealed IMI 318 at R O.1.

The growth rates in the  $\beta$  heat treated IMI 318 are compared in Fig. 10 with those for the thermal stress free IMI 685 as a function of  $\Delta K$ . This suggests that IMI 685 has greater fatigue crack growth resistance than the IMI 318 after the same heat treatment. Higher crack closure loads were found in the IMI 685 however, and when the results are re-presented in Fig. 11 in terms of  $\Delta K$  effective 2 the two alloys are shown to have similar growth rates. The different levels of crack closure load are assumed to arise from a difference in size of the components of the microstructure which in turn would produce a difference in the separation of the fracture faces at closure. This aspect of the closure model is currently being examined and the critical component of the microstructure has not yet been established.

The work indicates however, that the influence of closure must be considered when interpreting fatigue crack growth data obtained at low mean stresses from  $\beta$  heat treated titanium alloys and materials with similarly irregular fracture paths.

CONCLUSIONS

- 1) A substantial level of crack closure can occur during fatigue crack growth in  $\beta$  heat treated titanium alloy and this is not a surface effect.
- 2) The interaction between crack closure and thermally induced internal stresses can produce scatter in crack growth data.

- 3) Crack closure can result in a range of crack growth rates for tests at different R ratios.
- 4) In the absence of closure effects, similar intermediate fatigue crack growth rates are found for furnace cooled and oil quenched microstructures in IMI 685.
- 5) Crack closure occurs due to mismatch across the fracture faces produced by the irregular and branched crack path in  $\beta$  heat treated titanium alloy and is anticipated in other materials with similar fatigue fractures.
- 6) Scatter in the crack growth data may be rationalized by an effective  $\Delta K$  parameter.
- 7) The fatigue crack growth resistance of mill annealed IMI 318 is less than that of the same alloy after  $\beta$  heat treatment and the difference is only partly explained by crack closure.
- 8) Differences in crack growth rates between the  $\beta$  heat treated alloys IMI 318 and IMI 685 can be rationalized in terms of crack closure.

## ACKNOWLEDGEMENTS

The author acknowledges the help given by Dr. C.J. Beevers in discussions during the course of this work and the provision of laboratory facilities by Professor R.E. Smallman. The work was in large part financed by the Procurement Executive, Ministry of Defence.

## REFERENCES

- Chesnutt, J.C., C.G. Rhodes, and J.C. Williams (1976). Relationship between mechanical properties, microstructure, and fracture topography in  $\alpha+\beta$  titanium alloys. In Fractography-Microscopic Cracking Processes, ASTM STP 600. American Society for Testing and Materials, Philadelphia. pp. 99-138.
- Elber, W. (1970). Fatigue crack closure under cyclic tension. Eng. Frac. Mech., 2, 37-45.
- Evans, W.J. (1973). The effect of microstructure on fatigue crack propagation in  $\alpha+\beta$  titanium alloys. In The Practical Implications of Fracture Mechanisms. The Institution of Metallurgists, London. pp. 153-156.
- Evans, W.J., and A.W. Beale (1978). Fatigue crack propagation in wrought titanium alloys. In Forging and Properties of Aerospace Materials. The Metals Society, London. pp. 170-191.
- Eylon, D., and P.J. Bania (1978). Fatigue cracking characteristics of  $\beta$ -annealed large colony Ti-11 alloy. Met. Trans., 9A, 1273-1279.
- Eylon, D., J.A. Hall, C.M. Pierce, and D.L. Ruckle (1976). Microstructure and mechanical properties relationships in the Ti-11 alloy at room and elevated temperature. Met. Trans., 7A, 1817-1826.
- Halliday, M.D., and C.J. Beevers (1979). Non-closure of cracks and fatigue crack growth in  $\beta$  heat treated Ti-6Al-4V. Int. J. of Frac., 15, R27-R30.
- Harrigan, M.J., M.P. Kaplan, and A.W. Sommer (1974). Effect of chemistry and heat treatment on the fracture properties of Ti-6Al-4V alloy. In Fracture Prevention and Control. American Society for Metals, Ohio. pp. 225-253.
- Neal, D.F. (1978). A comparison of structure and properties of similarly processed  $\alpha+\beta$  and near  $\alpha$  titanium alloys. In Forging and Properties of Aerospace Materials. The Metals Society, London. pp. 199-216.
- Paris, P., and F. Erdogan (1963). A critical analysis of crack propagation laws. J. of Basic Eng., 85, 528-534.
- Paton, N.E., J.C. Williams, J.C. Chesnutt, and A.W. Thompson (1975). The effects of microstructure on the fatigue and fracture of commercial titanium alloys. In Specialists Meeting on Alloy Design for Fatigue and Fracture Resistance. Advisory Group for Aerospace Research and Development, NATO. pp. 4.1-4.14.
- Postans, P.J., and R.H. Jeal (1978). Dependence of crack growth performance upon structure in  $\beta$  processed titanium alloys. In Forging and Properties of Aerospace Materials. The Metals Society, London. pp. 192-198.

- Yoder, G.R., L.A. Cooley, and T.W. Crooker (1977). Observations on microstructurally sensitive fatigue crack growth in Widmanstätten Ti-6Al-4V alloy. Met. Trans., 8A, 1737-1743.
- Yoder, G.R., L.A. Cooley, and T.W. Crooker (1977). Enhancement of fatigue crack growth and fracture resistance in Ti-6Al-4V and Ti-6Al-6V-2Sn through microstructural modification. J. of Eng. Mat. and Tech., 99, 313-318.
- Yoder, G.R., L.A. Cooley, and T.W. Crooker (1979). 50-fold difference in region-II fatigue crack propagation resistance of titanium alloys: a grain size effect. J. of Eng. Mat. and Tech., 101, 86-90.
- Yoder, G.R., L.A. Cooley, and T.W. Crooker (1979). Quantitative analysis of microstructural effects on fatigue crack growth in Widmanstätten Ti-6Al-4V and Ti-8Al-1Mo-1V. Eng. Frac. Mech., 11, 805-816.
- Walker, N., and C.J. Beevers (1979). A fatigue crack closure mechanism in titanium. Fatigue of Eng. Mat. and Structures, 1, 135-148.